Supplemental Material for:
Frustration elimination and excited state search in coherent Ising machines

Zheng-Yang Zhou,[1,2] Clemens Gneiting,[2,3] J. Q. You,[4,5,*] and Franco Nori[2,3,6,†]

[1]*Zhejiang Key Laboratory of Quantum State Control and Optical Field Manipulation, Department of Physics, Zhejiang Sci-Tech University, Hangzhou 310018, China*

[2]*Theoretical Quantum Physics Laboratory, Cluster for Pioneering Research, RIKEN, Wakoshi, Saitama 351-0198, Japan*

[3]*Center for Quantum Computing, RIKEN, Wakoshi, Saitama 351-0198, Japan*

[4]*Zhejiang Key Laboratory of Micro-Nano Quantum Chips and Quantum Control, School of Physics, School of Physics, and State Key Laboratory for Extreme Photonics and Instrumentation, Zhejiang University, Hangzhou 310027, China*

[5]*College of Optical Science and Engineering, Zhejiang University, Hangzhou 310027, China*

[6]*Physics Department, The University of Michigan, Ann Arbor, Michigan 48109-1040, USA*

[*]jqyou@zju.edu.cn

[†]fnori@riken.jp

I. MAPPING ISING MODELS TO COHERENT ISING MACHINES

The basic structure of a CIM is a fiber cavity complemented by a nonlinear crystal and a coupling module. Optical pulses propagate in the cavity and form degenerated optical parametric oscillators (DOPOs) described by a two-photon pump (in the interaction picture),

$$H = -iS\sum_{n}[(a_n^\dagger)^2 - (a_n)^2], \tag{S1}$$

and loss terms including two-photon loss,

$$\mathcal{L}_{\rm tp}(\rho) = \sum_{n}\frac{\Gamma_{\rm tp}}{2}[2a_na_n\rho(t)a_n^\dagger a_n^\dagger - \{a_n^\dagger a_n^\dagger a_na_n, \rho(t)\}], \tag{S2}$$

and single-photon loss,

$$\mathcal{L}_{\rm s}(\rho) = \sum_{n}\frac{\Gamma_{\rm s}}{2}[2a_n\rho(t)a_n^\dagger - \{a_n^\dagger a_n, \rho(t)\}], \tag{S3}$$

where a_n is the annihilation operator of the nth DOPO mode, $\{\bullet, \bullet\}$ denotes the anti-commutator, and ρ is the density matrix describing all the DOPO modes. The DOPO exhibits a phase transition at

$$2|S| = \Gamma_s, \tag{S4}$$

where the steady-state transitions from a squeezed vacuum state to two possible coherent states [1, 2]:

$$|\Psi(t\to\infty)\rangle = |\pm\alpha\rangle. \tag{S5}$$

CIMs use these two coherent states to emulate spin states:

$$|\alpha\rangle \longleftrightarrow |\uparrow\rangle, \quad |-\alpha\rangle \longleftrightarrow |\downarrow\rangle. \tag{S6}$$

If there are N DOPO pulses in the CIM, the steady state is a collective mode corresponding to a many-body spin system, e.g.,

$$|\alpha\rangle\otimes|-\alpha\rangle\cdots\otimes|\alpha\rangle \longleftrightarrow |\uparrow\rangle\otimes|\downarrow\rangle\cdots\otimes|\uparrow\rangle.$$

Note that a DOPO exhibits dark states if the single-photon loss rate is vanishing ($\Gamma_{\rm s} \approx 0$):

$$|\Psi(t \to \infty)\rangle = C_+|\alpha\rangle + C_-|-\alpha\rangle, \tag{S7}$$

and the complex amplitude α of the coherent states is given by $\alpha = i\sqrt{2S/\Gamma_{\rm d}}$.

Two common design principles for implementing the optical coupling in CIMs are the optical delay-line architecture [3] and the measurement-feedback architecture [4], respectively. The optical delay-line coupling between two DOPO modes can be described by a collective loss,

$$\begin{aligned}\mathcal{L}_{m,n}(\rho) &= \frac{\Gamma_{\rm c}}{2}(2L_{n,m}\rho L_{n,m}^\dagger - L_{n,m}^\dagger L_{n,m}\rho - \rho L_{n,m}^\dagger L_{n,m}),\\ L_{n,m} &= a_n + \mathrm{sign}(J_{m,n})a_m.\end{aligned} \tag{S8}$$

where n and m correspond to two different DOPO modes. This phase-dependent loss in Eq. (S8) can be associated with an Ising interaction term:

$$H_{n,m} = J_{m,n}\sigma_z^{(n)}\sigma_z^{(m)}, \tag{S9}$$

where $\sigma_z^{(n)}$ is the Pauli matrix of the nth spin, and the coupling strength satisfies $|J_{m,n}| = J$. The effect of the collective loss and of the Ising interaction, respectively, are summarized in the following table:

	Effect	States	Values
Collective loss	Photon loss probability	$\|\alpha\rangle_n \otimes \|\alpha\rangle_m$	$2\|\alpha_n\|^2\Gamma_{\rm c}(1+\mathrm{sign}(J_{m,n}))$
		$\|\alpha\rangle_n \otimes \|-\alpha\rangle_m$	$2\|\alpha_n\|^2\Gamma_{\rm c}(1-\mathrm{sign}(J_{m,n}))$
		$\|-\alpha\rangle_n \otimes \|-\alpha\rangle_m$	$2\|\alpha_n\|^2\Gamma_{\rm c}(1+\mathrm{sign}(J_{m,n}))$
		$\|-\alpha\rangle_n \otimes \|\alpha\rangle_m$	$2\|\alpha_n\|^2\Gamma_{\rm c}(1-\mathrm{sign}(J_{m,n}))$
Ising interaction	Energy shift	$\|\uparrow\rangle_n \otimes \|\uparrow\rangle_m$	$J_{m,n}$
		$\|\uparrow\rangle_n \otimes \|\downarrow\rangle_m$	$-J_{m,n}$
		$\|\downarrow\rangle_n \otimes \|\downarrow\rangle_m$	$J_{m,n}$
		$\|\downarrow\rangle_n \otimes \|\uparrow\rangle_m$	$-J_{m,n}$

It is straightforward to see that the energy difference in the spin system is mapped to the loss difference in DOPO modes. An Ising energy $-J$ corresponds to vanishing loss, while an Ising energy J corresponds to finite loss. Due to the loss-dependent phase transition in Eq. (S4), the Ising ground state is mapped to a collective DOPO mode with lowest transition pump strength $|S|$.

The measurement-feedback coupling can be expressed as classical pumps on different DOPO modes:

$$H_{\rm MF} \; = \; -i\sum_{n,m}\Omega \;{\rm sign}(J_{n,m})\langle(a_m+a_m^\dagger)\rangle(a_n-a_n^\dagger). \tag{S10}$$

Such a pump can effectively modify the two-photon pump strength S in the semiclassical limit (mean field):

$$\begin{aligned} H+H_{\rm MF} \; &= \; -iS\sum_n[(a_n^\dagger)^2-(a_n)^2]-i\sum_{n,m}\Omega \;{\rm sign}(J_{n,m})\langle(a_m+a_m^\dagger)\rangle(a_n-a_n^\dagger) \\ &\approx \; -i\sum_n[S\langle(a_n+a_n^\dagger)\rangle-\sum_m\Omega \;{\rm sign}(J_{n,m})\langle(a_m+a_m^\dagger)\rangle](a_n^\dagger-a_n). \end{aligned} \tag{S11}$$

As the steady states of DOPOs are coherent states with 0 phase or π phase, we have

$$\langle(a_n+a_n^\dagger)\rangle=\pm\langle(a_m+a_m^\dagger)\rangle,$$

in the semi-classical limit. Here, we assume a negative S to make the amplitude α real. If

$$\langle(a_n+a_n^\dagger)\rangle={\rm sign}(J_{n,m})\langle(a_m+a_m^\dagger)\rangle,$$

the total pump strength acting on the nth mode is increased. For an opposite relative phase

$$\langle(a_n+a_n^\dagger)\rangle=-{\rm sign}(J_{n,m})\langle(a_m+a_m^\dagger)\rangle,$$

the total pump strength acting on the nth mode is reduced. According to the threshold relation in Eq. (S4), modifying the pump strength of the collective mode is equivalent to modifying the loss of the collective mode. Therefore, the measurement-feedback in Eq. (S11) can also be mapped to the Ising interaction.

II. PROBLEMS CAUSED BY FRUSTRATION

A. Intrinsic loss

In the collective loss coupling protocol, the Ising energy is mapped to the loss. Note that a collective loss with zero loss (that is, the system is in a dark state) corresponds to a spin configuration in which all the Ising coupling terms contribute negative energies. Such spin configurations do not exist in frustrated Ising models. Therefore, there will be intrinsic loss caused by the coupling protocol, if we use CIMs to simulate frustrated Ising models. Such intrinsic loss generically destroys most strong quantum effects, and thus prevents CIMs benefiting from quantum effects. Note that the current measurement-feedback coupling protocol exhibits few quantum effects.

B. Inhomogeneity in amplitudes

Although the current CIMs mainly work in the semi-classical regime, frustration can still cause problems. To correctly map an Ising model to a CIM, the amplitudes of different steady-state DOPO pulses are required to be the same. To see how inhomogeneous amplitudes can cause errors, let us, for example, consider a pair of spins,

$$|\uparrow\rangle_n \otimes |\uparrow\rangle_m,$$

which has the Ising coupling energy $-J$ for the coupling term

$$H_{n,m} = -J\sigma_z^n \sigma_z^m.$$

However, the collective DOPO mode

$$|\alpha\rangle_n \otimes |\alpha + \Delta\rangle_m,$$

is not a dark mode of the collective loss operator,

$$L_{n,m} = a_n - a_m.$$

In addition the effective pump strength shift in Eq. (S11) requires that

$$|\langle(a_m + a_m^\dagger)\rangle| = |\langle(a_n + a_n^\dagger)\rangle|.$$

Note that one possible approach to mitigate the problem of inhomogeneous amplitudes is the chaotic amplitude control [5].

III. POTENTIAL ADVANTAGES OF QUANTUM STATES IN A CIM

The advantages of quantum states for metrology have been analytically proved in spin systems [6]. Following the idea of spin systems, we show the potential advantages of quantum final states in CIMs. Consider an Ising problem with N_{solution} degenerate ground states and the corresponding optical states in a CIM

$$|\Psi_n\rangle, \quad 0 \leq n < N_{\text{solution}}. \tag{S12}$$

Due to the presence of N_{solution} degenerate ground states, the probability of obtaining a specific solution is

$$P = \frac{1}{N_{\text{solution}}}. \tag{S13}$$

Therefore, it is hard to verify the correctness of a candidate solution $|\psi_{\text{can}}\rangle$ if the CIM produces a mixture of the solution states $|\Psi_n\rangle$. Now we consider a superposition of all the ground states,

$$|\Psi\rangle = \frac{1}{\sqrt{N_{\text{solution}}}} \sum_n |\Psi_n\rangle. \tag{S14}$$

Here, the overlap between different effective spin states in CIMs is assumed to be negligible $\langle\Psi_n|\Psi_m\rangle \approx 0$ for $n \neq m$. Assume now that we have obtained N_{det} determined ground states $|\Psi_{n,\text{det}}\rangle$ with $n < N_{\text{det}}$. We can then prepare a superposition of all these determined ground states,

$$|\Psi_{\text{det}}\rangle = \frac{1}{\sqrt{N_{\text{det}}}} \sum_n |\Psi_{n,\text{det}}\rangle, \tag{S15}$$

and use the coherence between different solutions to verify the correctness of the candidate state

$$P_{\text{co}} = \langle\Psi_{\text{det}}|\Psi\rangle\langle\Psi|\Psi_{\text{can}}\rangle + \langle\Psi_{\text{can}}|\Psi\rangle\langle\Psi|\Psi_{\text{det}}\rangle = \frac{2\sqrt{N_{\text{det}}}}{N_{\text{solution}}}. \tag{S16}$$

We find that the coherence has a higher probability to be measured compared to the projection measurement with the success probability $1/N_{\text{solution}}$.

IV. THE IDEA OF THE ANCILLARY-MODE CONSTRUCTION

Here we introduce the basic idea behind introducing ancillary modes in dissipative coupling channels. Consider the collective coupling illustrated in Fig. S1(a), which can be expressed by the Lindblad operator,

$$L = a_1 + a_2. \tag{S17}$$

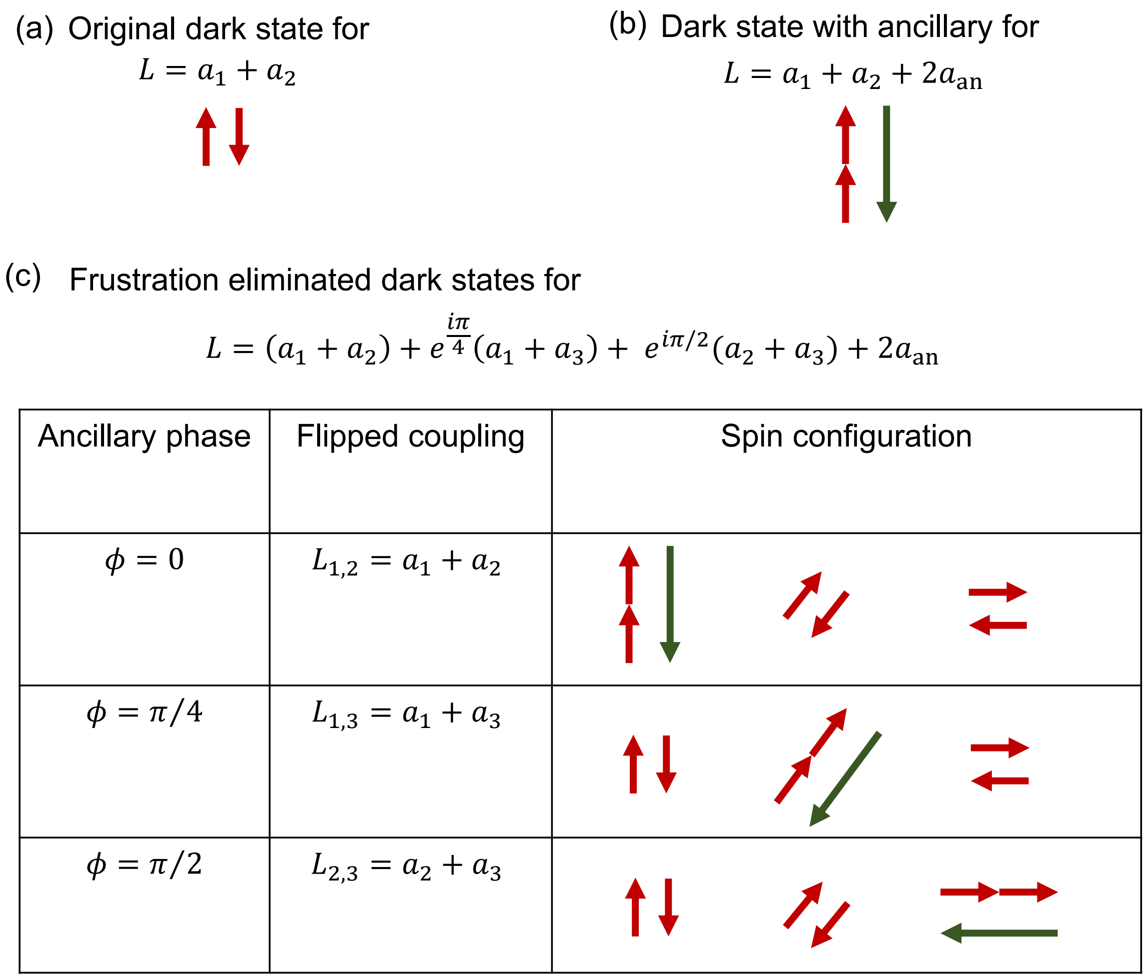

FIG. S1: Illustration of the ancillary-controlled coupling flipping.

When the two effective spins have opposite orientations, they cancel in the loss channel and form a dark mode, as illustrated in Fig. S1(a). On the other hand, the collective modes associated to aligned orientations couple to the loss channel, so that this alignment is suppressed by the dissipative coupling. This way, the dissipative coupling in Fig. S1(a) induces an antiferromagnetic coupling.

The preferred collective spin state can be modified by adding an additional ancillary mode, as illustrated in Fig. S1(b),

$$L' = a_1 + a_2 + 2a_{\rm an}. \tag{S18}$$

Due to the presence of a "larger" ancillary spin, the two signal spins must have the same orientation for all three spins to form a dark mode. In the new dark mode the two signal spins have the same orientation, as illustrated in Fig. S1(b). Note that the original dark mode $(a_1 - a_2)/\sqrt{2}$ is still decoupled from the loss channel in Fig. S1(b), but the original bright mode $(a_1 + a_2)/\sqrt{2}$ is now pumped by the ancillary mode $a_{\rm an}$. This can be verified as follows,

$$
\begin{aligned}
\frac{\partial\langle a_1+a_2\rangle}{\partial t} &= -i\langle [H,\rho](a_1+a_2)\rangle + \langle \mathcal{L}_{\rm tp}(\rho)(a_1+a_2)\rangle \\
&\quad + \frac{\Gamma_{\rm c}}{2}\langle (2L'\rho L'^{\dagger} - L'^{\dagger}L'\rho - \rho L'^{\dagger}L')(a_1+a_2)\rangle \\
&= -i\langle [H,\rho](a_1+a_2)\rangle + \langle \mathcal{L}_{\rm tp}(\rho)(a_1+a_2)\rangle \\
&\quad + \frac{\Gamma_{\rm c}}{2}[\langle L'\rho L'^{\dagger}(a_1+a_2)\rangle - \langle L'^{\dagger}L'\rho(a_1+a_2)\rangle + \langle L'\rho L'^{\dagger}(a_1+a_2)\rangle - \langle \rho L'^{\dagger}L'(a_1+a_2)\rangle] \\
&= -i\langle [H,\rho](a_1+a_2)\rangle + \langle \mathcal{L}_{\rm tp}(\rho)(a_1+a_2)\rangle \\
&\quad + \frac{\Gamma_{\rm c}}{2}[\langle L'\rho L'^{\dagger}(a_1+a_2)\rangle - \langle L'\rho(a_1+a_2)L'^{\dagger}\rangle + \langle \rho L'^{\dagger}(a_1+a_2)L'\rangle - \langle \rho L'^{\dagger}L'(a_1+a_2)\rangle] \\
&= -i\langle [H,\rho](a_1+a_2)\rangle + \langle \mathcal{L}_{\rm tp}(\rho)(a_1+a_2)\rangle \\
&\quad + \frac{\Gamma_{\rm c}}{2}[\langle L'\rho[L'^{\dagger},(a_1+a_2)]\rangle + \langle \rho L'^{\dagger}[(a_1+a_2),L']\rangle] \\
&= -i\langle [H,\rho](a_1+a_2)\rangle + \langle \mathcal{L}_{\rm tp}(\rho)(a_1+a_2)\rangle \\
&\quad + \frac{\Gamma_{\rm c}}{2}\langle (a_1+a_2+2a_{\rm an})\rho[(a_1^{\dagger}+a_2^{\dagger}+2a_{\rm an}^{\dagger}),(a_1+a_2)]\rangle \\
&\quad + \frac{\Gamma_{\rm c}}{2}\langle \rho(a_1^{\dagger}+a_2^{\dagger}+2a_{\rm an}^{\dagger})[(a_1+a_2),(a_1+a_2+2a_{\rm an})]\rangle \\
&= -i\langle [H,\rho](a_1+a_2)\rangle + \langle \mathcal{L}_{\rm tp}(\rho)(a_1+a_2)\rangle - \Gamma_{\rm c}(\langle a_1\rangle + \langle a_2\rangle + 2\langle a_{\rm an}\rangle).
\end{aligned}
\tag{S19}
$$

Note that the last term $-2\Gamma_{\rm c}\langle a_{\rm an}\rangle$ can be an effective pump if $\langle a_{\rm an}\rangle$ has the same sign as $-(\langle a_1\rangle + \langle a_2\rangle)$. Such an effective pump can cause the mode $(a_1 + a_2)$ to dominate the competition with the original dark mode $(a_1 - a_2)$, which is induced by the two-photon loss terms. Such a competition mechanism can be understood as follows,

$$
\begin{aligned}
\langle \mathcal{L}_{\rm tp}(\rho)(a_1+a_2)\rangle &= \frac{\Gamma_{\rm tp}}{2}\sum_{k=1,2}\langle a_k^2\rho[(a_k^{\dagger})^2,(a_1+a_2)]\rangle \\
&= -\Gamma_{\rm tp}\langle a_1^{\dagger}a_1^2\rangle - \Gamma_{\rm tp}\langle a_2^{\dagger}a_2^2\rangle \\
&= -\frac{\Gamma_{\rm tp}}{2\sqrt{2}}\langle (a_+^{\dagger}+a_-^{\dagger})(a_+ + a_-)^2\rangle - \frac{\Gamma_{\rm tp}}{2\sqrt{2}}\langle (a_+^{\dagger}-a_-^{\dagger})(a_+ - a_-)^2\rangle \\
&= -\frac{\Gamma_{\rm tp}}{2\sqrt{2}}\langle (a_+^{\dagger}a_+^2 + 2a_+^{\dagger}a_-a_+ + a_+^{\dagger}a_-^2)\rangle - \frac{\Gamma_{\rm tp}}{2\sqrt{2}}\langle (a_-^{\dagger}a_+^2 + 2a_-^{\dagger}a_-a_+ + a_-^{\dagger}a_-^2)\rangle \\
&\quad -\frac{\Gamma_{\rm tp}}{2\sqrt{2}}\langle (a_+^{\dagger}a_+^2 - 2a_+^{\dagger}a_-a_+ + a_+^{\dagger}a_-^2)\rangle + \frac{\Gamma_{\rm tp}}{2\sqrt{2}}\langle (a_-^{\dagger}a_+^2 - 2a_-^{\dagger}a_-a_+ + a_-^{\dagger}a_-^2)\rangle \\
&= -\frac{\Gamma_{\rm tp}}{\sqrt{2}}(\langle a_+^{\dagger}a_+^2\rangle + \langle a_+^{\dagger}a_-^2\rangle + \langle 2a_-^{\dagger}a_-a_+\rangle).
\end{aligned}
\tag{S20}
$$

with $a_+ = (a_1 + a_2)/\sqrt{2}$ and $a_- = (a_1 - a_2)/\sqrt{2}$. Under the mean field approximation, the last two terms describe single-photon loss acting on the mode a_+ with a loss rate depending on the semiclassical amplitude of the mode a_-. It follows that a_- is suppressed by a pumped a_+, even though it is decoupled from the loss.

To control multiple couplings with a single ancillary mode, we may associate different coupling terms with different phases and use a hyperspin as the ancillary mode, as illustrated in Fig. S1(c). The phase is an effective rotation of the z direction of each coupling term, so that different coupling terms do not interfere with each other. The hyperspin ancilla chooses a specific spin orientation, and flips the corresponding coupling term.

V. SEMICLASSICAL EQUATIONS FOR A CIM

In the limit of large amplitudes, we can also approximate a CIM with semiclassical equations of motion, which follow from a mean field approximation of the quantum dynamics:

$$\begin{aligned} \frac{\partial}{\partial t} A_n &= P A_n^* - \gamma_{\rm s} A_n - \gamma_{\rm d} A_n |A_n|^2 - C_n \\ C_n &= \sum_m |J_{n,m}| [A_n + \mathrm{sign}(J_{n,m}) A_m], \end{aligned} \tag{S21}$$

where $A_n \equiv \langle a_n \rangle$ is the amplitude of the nth mode with the annihilation operator a_n, and C_n is the coupling term determined by the coupling matrix $J_{n,m} = \pm J$ with $J > 0$. Without coupling $|J_{n,m}| = 0$, each mode in Eq. (S21) has two steady solutions $A_m = \pm\sqrt{(P - \gamma_{\rm s})/\gamma_{\rm d}}$, which correspond to two spin orientations, above the threshold $P > \gamma_{\rm s}$.

The coupling term C_n can shift the threshold as

$$P > \gamma_{\rm s} + \sum_m |J_{n,m}| + \sum_j J_{n,m} \frac{A_m}{A_n}. \tag{S22}$$

Note that $A_m/A_n = \pm 1$, if the amplitudes are homogeneous.

A. Semiclassical description for frustration elimination

The ancillary modes in the frustration-elimination method can be described by the following mean-field equations,

$$\begin{aligned} \frac{\partial}{\partial t} A_{\rm ans} &= 2 S A_{\rm ani}^* - \Gamma_{\rm tp} A_{\rm ans} |A_{\rm ani}|^2 - C_{\rm ans}, \\ \frac{\partial}{\partial t} A_{\rm ani} &= 2 S A_{\rm ans}^* - \Gamma_{\rm tp} A_{\rm ani} |A_{\rm ans}|^2 - C_{\rm ani}, \end{aligned} \tag{S23}$$

with $A_{\rm ans} \equiv \langle a_{\rm ans}\rangle$ and $A_{\rm ani} \equiv \langle a_{\rm ani}\rangle$. Note that the single-photon loss is omitted here. The dark mode condition for the ancillary modes is $A_{\rm ans}A_{\rm ani} = 2S/\Gamma_{\rm tp}$. With a pair of conjugate coupling terms $C_{\rm ans} = C^*_{\rm ani}$, the solutions obey the symmetry $A_{\rm ans} = A^*_{\rm ani}$, which is the condition required for the ancillary modes. Note that the Lindblad terms in the main text satisfy this relation.

The semiclassical coupling terms for the frustration elimination are

$$\begin{aligned} C^{\rm F}_i &= J^{\rm eff}_i(\tilde{A} + 2A_{\rm ans}) + J^{\rm eff*}_i(\tilde{A}^* + 2A_{\rm ani}), \\ C_{\rm ans} &= 2J\{\tilde{A} + 2A_{\rm ans}\}, \quad C_{\rm ani} = 2J\{\tilde{A}^* + 2A_{\rm ani}\}, \end{aligned} \tag{S24}$$

with $\tilde{A} = \sum_{n,m} e^{i\phi_{n,m}}[A_m + A_n]$, and the phase terms $\phi_{1,2} = 0$, $\phi_{2,3} = \pi/2$, $\phi_{1,3} = \pi/4$. Note that the effective coupling strength $J^{\rm eff}_i \equiv \sum_j(e^{-i\phi_{i,j}}J_{i,j} + e^{-i\phi_{j,i}}|J_{j,i}|)$, which has no effect on the dark-state condition $C^{\rm F}_i = 0$, originates from the quantum coupling model described by the Lindblad operator.

VI. REALIZATION OF FRUSTRATION-ELIMINATION-TYPE COLLECTIVE LOSS

A. Two-mode collective loss with optical delay lines

We first consider a two-mode collective loss formed by a delay line coupled to two optical pulses, as illustrated in Fig. S2,

The input mode $b_{\rm in}$ (usually the vacuum state) couples with two system modes successively through two beam splitters. The fields after the scattering in Fig. S2(a) are:

$$\begin{aligned} b'_{\rm in} &= Tb_{\rm in} + Ra_1, \\ a'_1 &= Ta_1 - Rb_{\rm in}. \end{aligned} \tag{S25}$$

After the second scattering, the fields are:

$$\begin{aligned} b''_{\rm in} &= T^2 b_{\rm in} + RTa_1 + Ra_2, \\ a'_1 &= Ta_1 - Rb_{\rm in}, \\ a'_2 &= Ta_2 - RTb_{\rm in} - R^2 a_1. \end{aligned} \tag{S26}$$

Here, the transmission rate is T^2 and the reflection rate is R^2. When the transmission rate is close to 1, the input mode $b_{\rm in}$ is not coupled to the collective mode $(a_1 - a_2)$ up to the

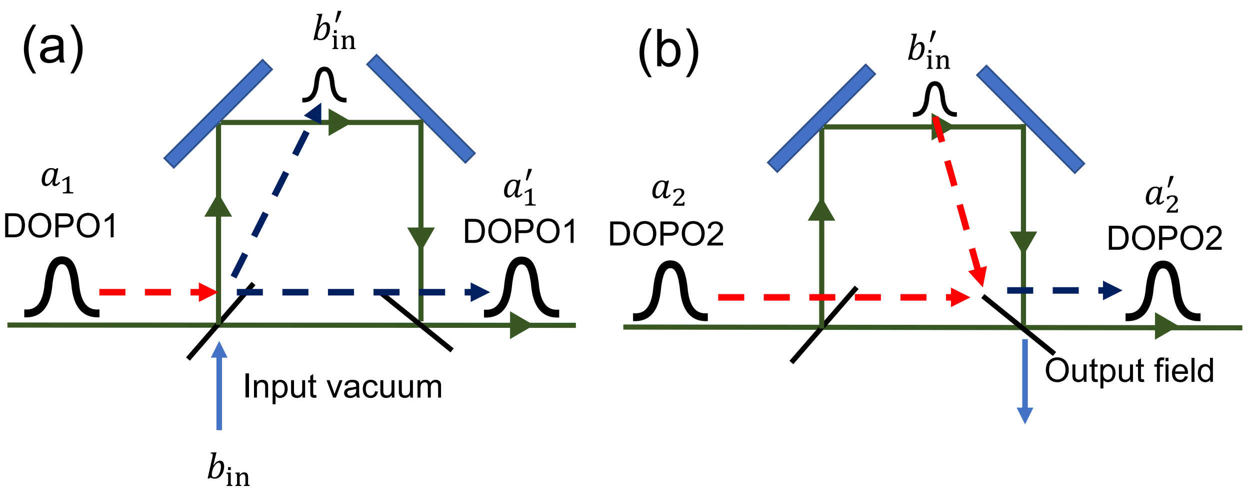

FIG. S2: Illustration of the collective loss realized through a delay-line coupling. (a) First, the first pulse denoted as a_1 passes the first beam splitter and mixes with a vacuum field denoted as $b_{\rm in}$ in the delay line denoted as $b'_{\rm in}$. (b) Then the pulse $b'_{\rm in}$, which carries the information of a_1, interacts with the second pulse a_2 at the second beam splitter. For a proper collective state, the output field is almost a vacuum state, which corresponds to a dark state of such collective loss.

second order of $|R|$. The change of the "dark mode" is as follows:

$$\begin{aligned} a'_1 - a'_2 &= T(a_1 - a_2) + (1-T)Rb_{\rm in} + R^2 a_1 \\ &= (T + 0.5R^2)(a_1 - a_2) + (1-T)Rb_{\rm in} + 0.5R^2(a_1 + a_2). \end{aligned} \tag{S27}$$

It is easy to see that this "dark mode" is not really dark, but coupled to the bright mode $(a_1 + a_2)$ up to second order in R. Therefore, we can conclude that the "dark mode" in Fig. S2(a) is dark to the input field $b_{\rm in}$, but not completely decoupled from other modes. Note that the second order of R is important because the loss generated by the delay line on the bright mode is of the order of R^2.

To solve this problem, we can introduce a delay line with opposite scattering order, as shown in Fig. S3. Such a delay line has the following effects on the DOPO pulses:

$$\begin{aligned} a''_2 &= Ta'_2 - Rb_{\rm in,op}, \\ a''_1 &= Ta'_1 - RTb_{\rm in,op} - R^2 a'_2. \end{aligned} \tag{S28}$$

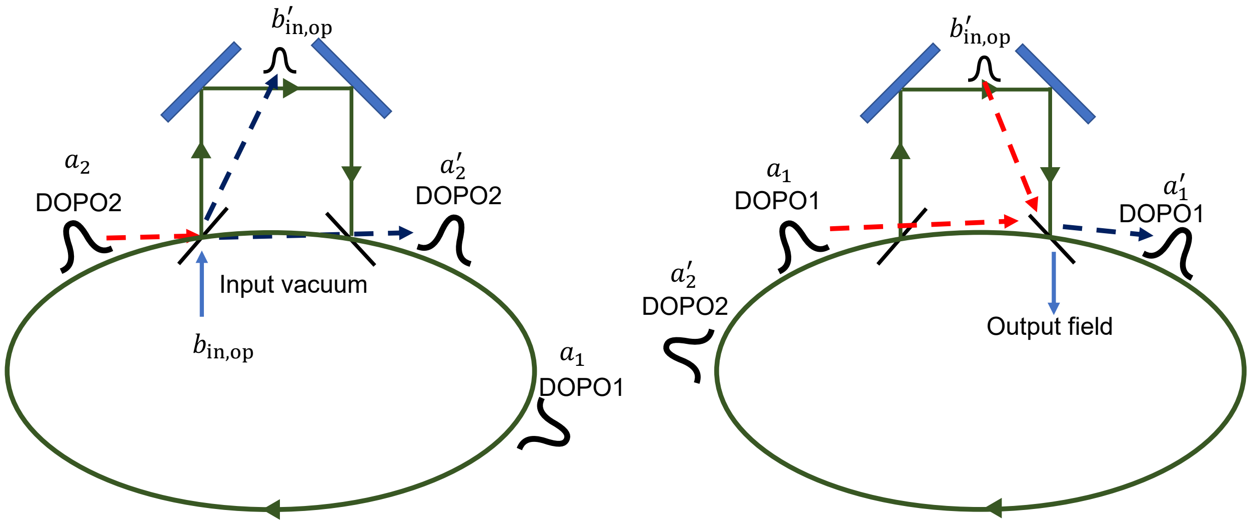

FIG. S3: Illustration of the open-port delay line in the opposite direction. A delay line can only delay and convey the information of a pulse to the pulses coming after it. However, note that in cyclic structures, e.g., in CIMs, the nth pulse in the mth circle passes the coupling modula before the $(n-1)$th pulse in the $(m+1)$th circle. Therefore, a delay line in the opposite direction delays the pulses longer than the circling period.

The total effects of the two delay lines are:

$$\begin{aligned} a_1'' &= T^2 a_1 - T^3 R b_{\text{in}} - RT b_{\text{in,op}} - R^2 T a_2 + R^4 a_1, \\ a_2'' &= T^2 a_2 - T^2 R b_{\text{in}} - T R^2 a_1 - R b_{\text{in,op}}. \end{aligned} \tag{S29}$$

After passing the two-delay lines with opposite scattering order, the collective mode $(a_1 - a_2)$ becomes,

$$\begin{aligned} a_1'' - a_2'' &= T(T+R^2)(a_1 - a_2) - RT^2(T-1)b_{\text{in}} - R(T-1)b_{\text{in,op}} + R^4 a_1 \\ &\approx (a_1 - a_2) + o(R^2). \end{aligned} \tag{S30}$$

This collective mode is unchanged up to second order in T. Therefore, two delay lines with different directions can form a dark mode. The collective mode with opposite relative phase $(a_1 + a_2)$ experiences loss through these delay lines:

$$\begin{aligned} a_1'' + a_2'' &= T(T-R^2)(a_1 + a_2) - RT^2(T+1)b_{\text{in}} - R(T+1)b_{\text{in,op}} + R^4 a_1 \\ &\approx (1-R^2)(a_1 + a_2) - R(b_{\text{in}} + b_{\text{in,op}}) + o(R^2). \end{aligned} \tag{S31}$$

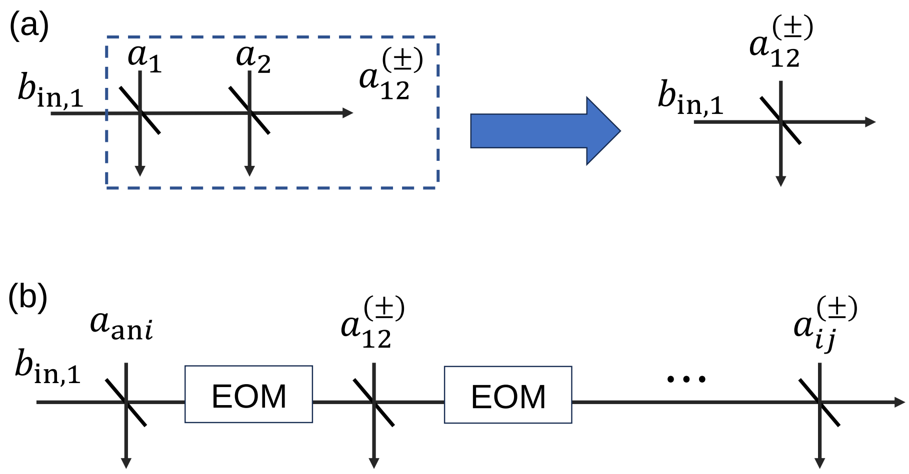

FIG. S4: Illustration of the multi-port delay line. (a) Expression of two modes coupled to a delay line as a collective mode. (b) Illustrations of phase terms in the frustration-eliminating channel generated by the phase and amplitude modulators (EOM). A multi-port delay line can be naively interpreted as connecting several two-port delay lines with EOMs.

Note that Eq. (S31) is equivalent to the coupling between a loss channel $b_{\mathrm{in}} + b_{\mathrm{in,op}}$ and a collective mode $(a_1 + a_2)$. The collective loss Eq. (S31) can also be expressed by the Lindblad terms:

$$\begin{aligned} \mathcal{L}_{1,2}(\rho) &= \frac{\Gamma_c}{2}(2L_{1,2}\rho L_{1,2}^\dagger - L_{1,2}^\dagger L_{1,2}\rho - \rho L_{1,2}^\dagger L_{1,2}), \\ L_{1,2} &= a_1 + a_2. \end{aligned} \tag{S32}$$

Note that the preferred collective mode can be changed by including an electro-optic phase and amplitude modulator (EOM),

$$L_{1,2} = a_1 + a_2 \longrightarrow L'_{1,2} = a_1 - a_2. \tag{S33}$$

B. Multi-mode collective loss for frustration elimination

To eliminate the frustration in CIMs, we need a frustration-eliminating loss channel of the following form:

$$L_{\mathrm{ani}} = \sum_{n,m} e^{i\phi_{m,n}}(a_n + \mathrm{sign}(J_{m,n})a_m) + 2a_{\mathrm{ani}}. \tag{S34}$$

Note that here we take the frustration-eliminating channel of an idler ancillary mode as an example, while the channel for the signal ancillary modes only differs in the phases. Such loss can be realized by multi-port delay lines, as illustrated in Fig. S4.

To simplify the expressions, we express the two signal modes coupled to the delay line in Fig. S2 as a collective mode, as shown in Fig. S4(a). Note that

$$a_{12}^{(\pm)} = a_1 \pm a_2. \tag{S35}$$

We can couple multiple collective modes, which correspond to different coupling terms in Eq. (S8), to a common open-port delay, as illustrated in Fig. S4(b). By introducing necessary phase terms $\phi_{m,n}$ with EOMs, the collective mode coupled to the delay line is exactly the Lindblad operator in Eq. (S34). The additional coupling terms can be cancelled by a delay line in opposite direction as illustrated in Fig. S5.

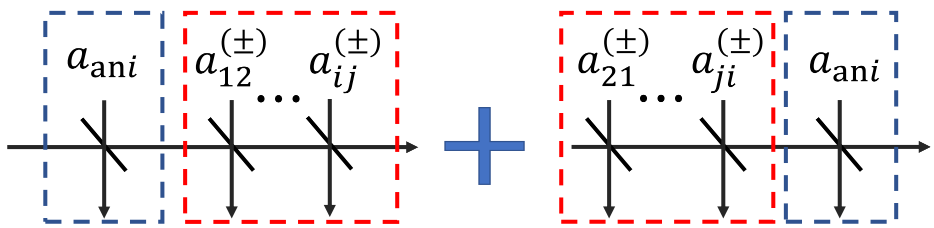

FIG. S5: Illustration of the frustration-eliminating loss channel formed by a pair of multi-port delay lines. As in the two-port delay cases, the unwanted coupling terms can be eliminated with a delay line in opposite direction.

VII. FRUSTRATION ELIMINATION IN MEASUREMENT-FEEDBACK COUPLING

Following the idea in Eq. (S11), the frustration-elimination coupling can also be realized with measurement feedback.

$$H_{\text{FEMF}} = i\Omega\langle(L_{\text{ani}} + L_{\text{ani}}^{\dagger})\rangle(L_{\text{ani}} - L_{\text{ani}}^{\dagger}). \tag{S36}$$

Consider now the semi-classical amplitude equation of the nth DOPO mode under the influence of this Hamiltonian,

$$\begin{aligned}\frac{\partial}{\partial t}\langle a_n\rangle &= i\langle[H_{\mathrm{FEMF}}, a_n]\rangle,\\ &= -\Omega\langle(L_{\mathrm{ani}}+L_{\mathrm{ani}}^{\dagger})\rangle\langle[(L_{\mathrm{ani}}-L_{\mathrm{ani}}^{\dagger}), a_n]\rangle \end{aligned} \tag{S37}$$

Note that the contribution of the frustration-elimination loss in Eq. (S34) to the amplitude equation has a similar form in the semi-classical limit,

$$\begin{aligned}\frac{\partial}{\partial t}\langle a_n\rangle &= \frac{\Gamma_{\mathrm{c}}}{2}\langle a_n(2L_{\mathrm{ani}}\rho L_{\mathrm{ani}}^{\dagger} - L_{\mathrm{ani}}^{\dagger}L_{\mathrm{ani}}\rho - \rho L_{\mathrm{ani}}^{\dagger}L_{\mathrm{ani}})\rangle,\\ &= \frac{\Gamma_{\mathrm{c}}}{2}\langle[a_n, L_{\mathrm{ani}}]\rho L_{\mathrm{ani}}^{\dagger}\rangle + \frac{\Gamma_{\mathrm{c}}}{2}\langle[L_{\mathrm{ani}}^{\dagger}, a_n]L_{\mathrm{ani}}\rho\rangle,\\ &\approx -\frac{\Gamma_{\mathrm{c}}}{2}\langle L_{\mathrm{ani}}+L_{\mathrm{ani}}^{\dagger}\rangle\langle[(L_{\mathrm{ani}}-L_{\mathrm{ani}}^{\dagger}), a_n]\rangle. \end{aligned} \tag{S38}$$

VIII. SCALING OF FRUSTRATION ELIMINATION DISSIPATIVE COUPLING

A. General design for scaling the frustration-elimination method

As mentioned in the main text, applying the frustration elimination method to the general case of flipping several couplings requires a modified model,

$$\begin{aligned} L_{\mathrm{ans}}^{n,m} &= L_{n,m} + i(b_{\mathrm{control}} + b_{n,m}) + 2a_{\mathrm{ans}}^{n,m},\\ L_{\mathrm{ani}}^{n,m} &= L_{n,m} - i(b_{\mathrm{control}} + b_{n,m}) + 2a_{\mathrm{ani}}^{n,m},\\ L_{\mathrm{control}} &= \sum b_{n,m} + (2N_{\mathrm{F}} - N_{\mathrm{c}})b_{\mathrm{control}}. \end{aligned} \tag{S39}$$

Unlike the single-ancilla case, now a pair of frustration eliminating loss channels is attributed to each coupling term $L_{m,n}$. Each pair of ancillary modes can either flip the corresponding loss term or the coupling between a pair of control modes b_{control} and $b_{n,m}$. If a coupling term $L_{n,m}$ is flipped, the corresponding control modes prefer the dark state of $(b_{\mathrm{control}} + b_{n,m})$. If we want to flip N_{F} couplings within all the N_{c} coupling terms, we need N_{F} control modes $b_{n,m}$ in the dark state of $(b_{\mathrm{control}} + b_{n,m})$ and $(N_{\mathrm{c}} - N_{\mathrm{F}})$ control modes in the dark state of

$(b_{\text{control}} - b_{n,m})$. Such control is achieved by the third line of Eq. (S39), which prefers N_{F} control modes $b_{n,m}$ to share the same orientation with the control mode b_{control}.

The basic idea is to control different coupling terms with different ancillary modes, and to control the number of active ancillary modes with additional loss channels. For each coupling term $L_{n,m}$ in the original Ising model, we need a pair of frustration-eliminating coupling channels, $L_{\text{ans}}^{n,m}$ and $L_{\text{ani}}^{n,m}$, which comprises three additional modes, i.e., $b_{n,m}$, $a_{\text{ans}}^{n,m}$ and $a_{\text{ani}}^{n,m}$. In addition to these ancillary modes distributed to each coupling term, we also need a control mode b_{control} to adjust the number of flipped couplings. Therefore, the relation between the total number of additional modes N_{ad} and the number of coupling terms N_{c} in the original model is

$$N_{\text{ad}} = 3N_{\text{c}} + 1. \tag{S40}$$

B. Semi-classical equations and error identification

Simulating the quantum model of frustration elimination is in general a challenge. Therefore, we alternatively use the following semi-classical equations under the mean-field approximation,

$$\frac{\partial A_i}{\partial t} \equiv \frac{\partial \langle a_i \rangle}{\partial t} \approx i\langle [H, a_i] \rangle - \sum_k \frac{\gamma_k}{2} \left[\langle [a_i, L_k^\dagger] \rangle \langle L_k \rangle - [a_i, L_k] \rangle \langle L_k^\dagger \rangle \right]. \tag{S41}$$

The equations for all the modes in Eq. (S39) are as follows,

$$
\begin{aligned}
\frac{\partial}{\partial t}A_n &= PA_n^* - \gamma_{\rm d}A_n|A_n|^2 - \gamma_{\rm c}\sum_{n>m}(A_n + C_{n,m}A_m + A_{\rm ans}^{n,m} + A_{\rm ani}^{n,m}) \\
&\quad -\gamma_{\rm c}\sum_{n<m}C_{n,m}(A_n + C_{n,m}A_m + A_{\rm ans}^{n,m} + A_{\rm ani}^{n,m}), \\
\frac{\partial}{\partial t}B_{n,m} &= PB_{n,m}^* - \gamma_{\rm d}B_{n,m}|B_{n,m}|^2 - \gamma_{\rm c}(B_{\rm control} + B_{n,m} - iA_{\rm ans}^{n,m} + iA_{\rm ani}^{n,m}) \\
&\quad -\frac{\gamma_{\rm c}}{2}\left[\sum_{l>m}B_{l,m} + (2N_{\rm F} - N_{\rm c})B_{\rm control}\right], \\
\frac{\partial}{\partial t}A_{\rm ans}^{n,m} &= PA_{\rm ani}^{n,m*} - \gamma_{\rm d}A_{\rm ans}^{n,m}|A_{\rm ani}^{n,m}|^2 - \gamma_{\rm c}(A_n + C_{n,m}A_j + iB_{\rm control} + iB_{n,m} + 2A_{\rm ans}^{n,m}), \\
\frac{\partial}{\partial t}A_{\rm ani}^{n,m} &= PA_{\rm ans}^{n,m*} - \gamma_{\rm d}A_{\rm ani}^{n,m}|A_{\rm ans}^{n,m}|^2 - \gamma_{\rm c}(A_n + C_{n,m}A_j - iB_{\rm n,m} - iB_{n,m} + 2A_{\rm ani}^{n,m}), \\
\frac{\partial}{\partial t}B_{\rm control} &= PB_{\rm control}^* - \gamma_{\rm d}B_{\rm control}|B_{\rm control}|^2 - \gamma_{\rm c}\sum_{n>m}(B_{\rm control} + B_{n,m} - iA_{\rm ans}^{n,m} + iA_{\rm ani}^{n,m}) - \\
&\quad (2N_{\rm F} - N_{\rm c})\gamma_{\rm c}\left[\sum_{l>m}B_{l,m} + (2N_{\rm F} - N_{\rm c})B_{\rm control}\right]. \qquad \text{(S42)}
\end{aligned}
$$

Here $A_n = \langle a_n \rangle$, $B_{n,m} = \langle b_{n,m} \rangle$, $B_{\rm control} = \langle b_{\rm control} \rangle$, $A_{\rm ani}^{n,m} = \langle a_{\rm ani}^{n,m} \rangle$, and $A_{\rm ans}^{n,m} = \langle a_{\rm ans}^{n,m} \rangle$.

Without frustration, the amplitudes of all modes should have the same absolute value. Therefore, we can use the amplitude inhomogeneity as an indicator for errors. We first define the average amplitude as

$$
\bar{A} = \frac{\sum_n |A_n| + \sum_{n,m}(|B_{n,m}| + |A_{\rm ans}^{n,m}| + |A_{\rm ani}^{n,m}|) + |B_{\rm control}|}{N + 3N_{\rm c} + 1}. \qquad \text{(S43)}
$$

The cumulative fluctuation of the amplitudes can then be defined as

$$
F = \sum_n (|A_n| - \bar{A})^2 + \sum_{n,m}[(|B_{n,m}| - \bar{A})^2 + (|A_{\rm ans}^{n,m}| - \bar{A})^2 + (|A_{\rm ani}^{n,m}| - \bar{A})^2] + (|B_{\rm control}| - \bar{A})^2. \qquad \text{(S44)}
$$

Note that this fluctuation contains the inhomogeneity in both signal modes and ancillary modes.

C. Additional numerical results

In the main text, we focus on a three-mode example, which is the simplest example of a frustrated Ising model. Here, we apply the frustration elimination and excited-state search to larger systems, see Figs. S6 and S7.

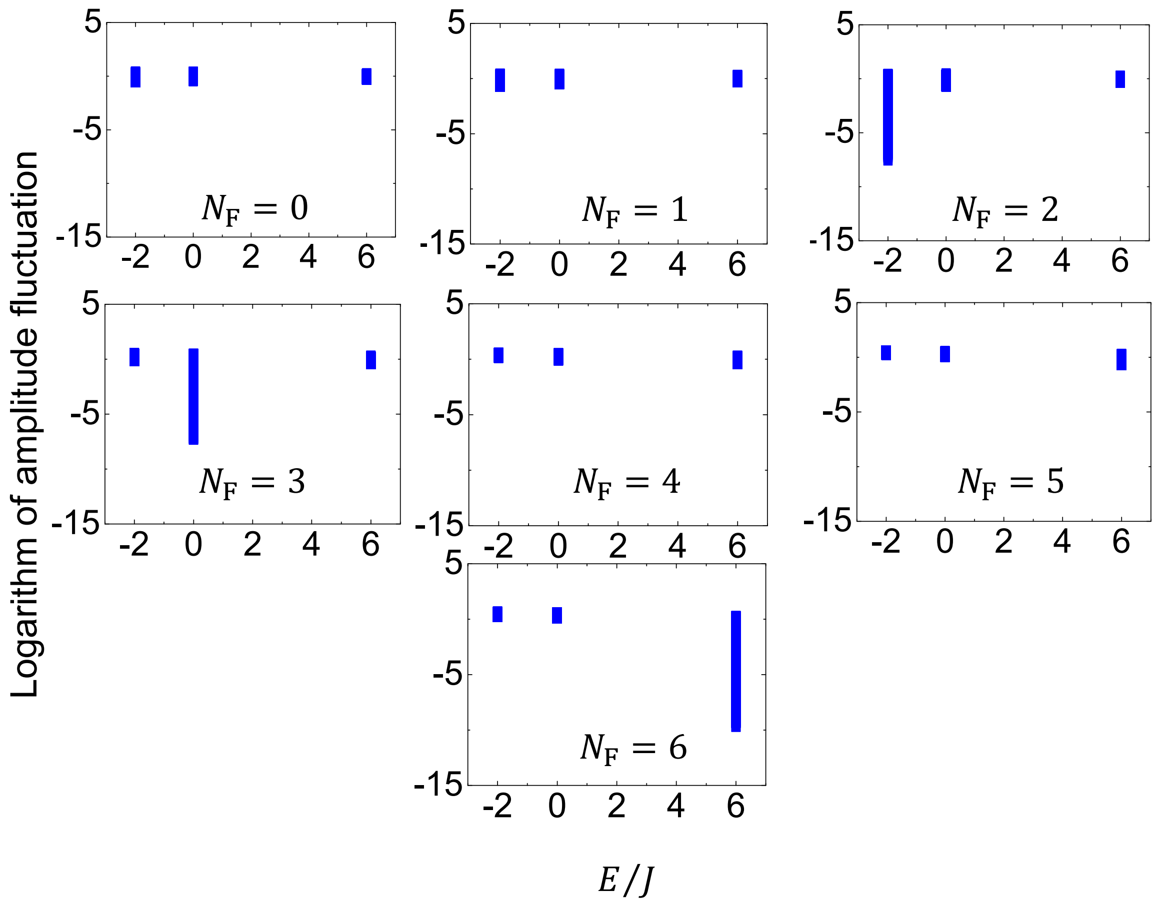

FIG. S6: Relation between the logarithm of the amplitude fluctuation and the Ising energy of the CIM states obtained with random initial conditions. The Ising model studied is a four-mode one with all-to-all antiferromagnetic coupling. The seven subfigures correspond to seven different numbers of flipped couplings. For $N_{\mathrm{F}} = 0, 1$, no solution is found due to the frustration. The system reaches frustration elimination, and the ground states are found for $N_{\mathrm{F}} = 2$. By further increasing N_{F}, the excited states with two different excited energies are found for $N_{\mathrm{F}} = 3$ and $N_{\mathrm{F}} = 6$.

We find that the vanishing fluctuation is also a sufficient condition for correct solutions for the four-mode case and the five-mode case. Therefore, the amplitude inhomogeneity can be used as an indicator for the wrong solutions. In addition, the excited states search is also effective in the examples studied here. By adding more flipped coupling terms, we can find the states with arbitrary energy, which is not possible in current CIMs.

To conclude, we remark that the probability to find correct solutions is reduced due to the additional ancillary modes. However, this reduction can be partially compensated by the self-checking functionality and the potential advantages brought by quantum effects. Presently, the main advantage of these ancillary modes in the semi-classical regime is the search for states with arbitrary energy.

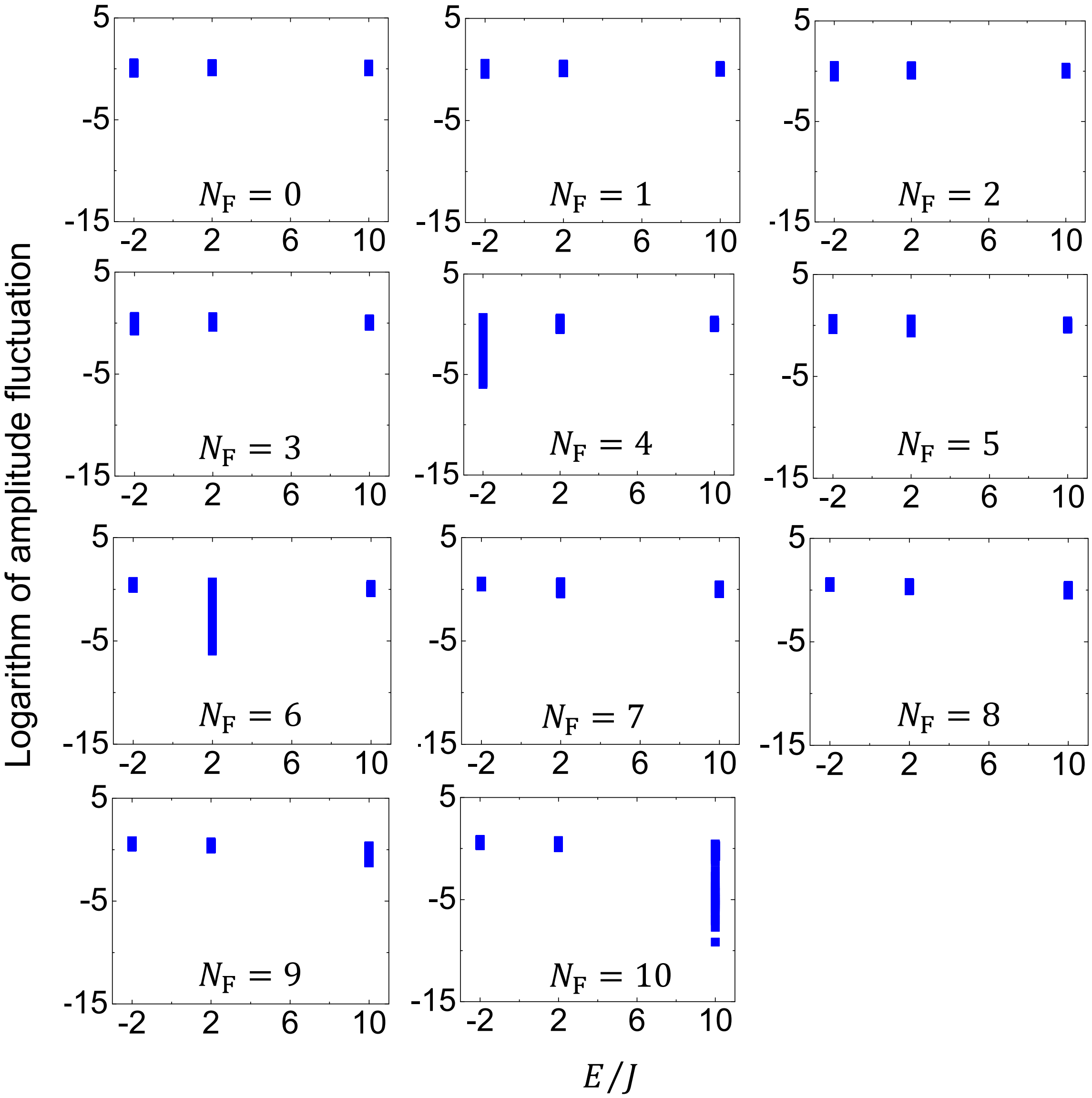

FIG. S7: Relation between the logarithm of the amplitude fluctuation and the Ising energy of the CIM states obtained with random initial conditions. The Ising model studied is a five-mode one with all-to-all antiferromagnetic coupling. The eleven subfigures correspond to eleven different numbers of flipped couplings. For $N_\mathrm{F} < 4$, no solution is found due to the frustration. The system reaches frustration elimination, and the ground states are found for $N_\mathrm{F} = 4$. By further increasing N_F, the excited states with two different excited energies are found for $N_\mathrm{F} = 6$ and $N_\mathrm{F} = 10$.

[1] M. Wolinsky and H. J. Carmichael, Phys. Rev. Lett. **60**, 1836 (1988), URL https://link.aps.org/doi/10.1103/PhysRevLett.60.1836.

[2] P. D. Drummond and K. Dechoum, Phys. Rev. Lett. **95**, 083601 (2005), URL https://link.aps.org/doi/10.1103/PhysRevLett.95.083601.

[3] A. Marandi, Z. Wang, K. Takata, R. L. Byer, and Y. Yamamoto, Nature Photonics **8**, 937 (2014), URL https://doi.org/10.1038/nphoton.2014.249.

[4] P. L. McMahon, A. Marandi, Y. Haribara, R. Hamerly, C. Langrock, S. Tamate, T. Inagaki, H. Takesue, S. Utsunomiya, K. Aihara, et al., Science **354**, 614 (2016).

[5] T. Leleu, Y. Yamamoto, P. L. McMahon, and K. Aihara, Phys. Rev. Lett. **122**, 040607 (2019), URL https://link.aps.org/doi/10.1103/PhysRevLett.122.040607.

[6] J. Ma, X. Wang, C. P. Sun, and F. Nori, Physics Reports **509**, 89 (2011), URL https://doi.org/10.1016/j.physrep.2011.08.003.